Lab on a Chip

RSC Publishing

PAPER

View Article Online
View Journal | View Issue

Cite this: *Lab Chip*, 2013, **13**, 3555

Skin and hair on-a-chip: *in vitro* skin models *versus ex vivo* tissue maintenance with dynamic perfusion†

Beren Ataç,‡[a] Ilka Wagner,‡[a] Reyk Horland,[a] Roland Lauster,[a] Uwe Marx,[a] Alexander G. Tonevitsky,[b] Reza P. Azar[c] and Gerd Lindner*[a]

Received 19th February 2013,
Accepted 1st May 2013

DOI: 10.1039/c3lc50227a

www.rsc.org/loc

Substantial progress has been achieved over the last few decades in the development of skin equivalents to model the skin as an organ. However, their static culture still limits the emulation of essential physiological properties crucial for toxicity testing and compound screening. Here, we describe a dynamically perfused chip-based bioreactor platform capable of applying variable mechanical shear stress and extending culture periods. This leads to improvements of culture conditions for integrated *in vitro* skin models, *ex vivo* skin organ cultures and biopsies of single hair follicular units.

Introduction

The majority of current commercially available skin equivalents are based on static culture systems emulating human epidermis only, or combining epidermis and dermis in so-called full-thickness skin equivalents (for reviews, see[1,2]). None of the existing systems comprise functional and (patho-) physiologically important elements, such as an immune system, vasculature or skin appendices.[3] Most of the skin-related pathologies, such as wound healing, skin tumours, psoriasis, contact allergies, androgenic alopecia, *etc.*, essentially require the elements mentioned above. Consequently, reproducible *in vitro* systems should reflect these circumstances.

Further bioengineering is particularly necessary for the implementation of adipose tissue, hair follicles and a functional vascular network.[4–7] Notably, adipose-derived stromal cells are not only important for lipid metabolism, but also have a major impact on the regulation of fibroblast and keratinocyte proliferation by cytokine secretion.[8] In addition, the hair follicle serves as a considerable storage area, takes a substantial role in skin metabolism, contains multiple stem cell lineages with regenerative capacity, and constitutes the major penetration route of topically applied substances to the skin.[9–11]

Native skin is supplied through a capillary network in the dermis, formed by endothelial cells. Therefore, endothelial cells have been integrated into the dermal portion of full-thickness skin substitutes.[12,6,7] However, because of the lack of shear stress in existing *in vitro* systems, no mature blood vessels have been produced and no skin substitute with an artificial blood stream at micro-scale has been described so far.

Such an improved skin equivalent needs to be implemented in a culture system which permits a constant oxygen and nutrient supply, measures and removes toxic metabolites, and can be intravitally monitored for sustainability over weeks and even months. This is necessary when it is used, for example, as a potential replacement of animal studies for repeated dermal toxicity assays, as required in OECD (Organisation for Economic Co-operation and Development) guidelines 410 and 411. We have recently successfully developed a PDMS-based microfluidic chip system with the dimensions of a conventional glass microscope slide[13,14] to function as a long-term dynamic bioreactor for various tissues. In this study, we used the chip-based system to prolong the maintenance and testing period of a commercially available skin equivalent (SE) and improve its nutritional and cellular deposit with *ex vivo* subcutaneous tissue (SCT). Furthermore, *ex vivo* skin and single hair follicular units (follicular unit extracts – FUEs) were cultured in the bioreactor platform to extend the static maintenance periods concerning substance testing.

Materials and methods

Device design and assembly

The bioreactor platform we developed (Fig. 1a), which will subsequently be referred as the ''MOC'' (Multi-Organ-Chip), provides a dynamically perfused micro-channel system com-

[a]*Technische Universität Berlin, Institute of Biotechnology, Berlin, Germany. E-mail: gerd.lindner@tu-berlin.de; Fax: +49 (0)30-314-27914; Tel: +49 (0)30-314-27910*

[b]*Institute of General Pathology and Pathophysiology Russian Academy of Medical Science, Moscow, Russia*

[c]*Zentrum für moderne Haartransplantation / Centre for Modern Hair Transplantation, Berlin, Germany*

† Conflict of interest disclosures: the authors declare no competing financial interests.

‡ These authors contributed equally to this work.

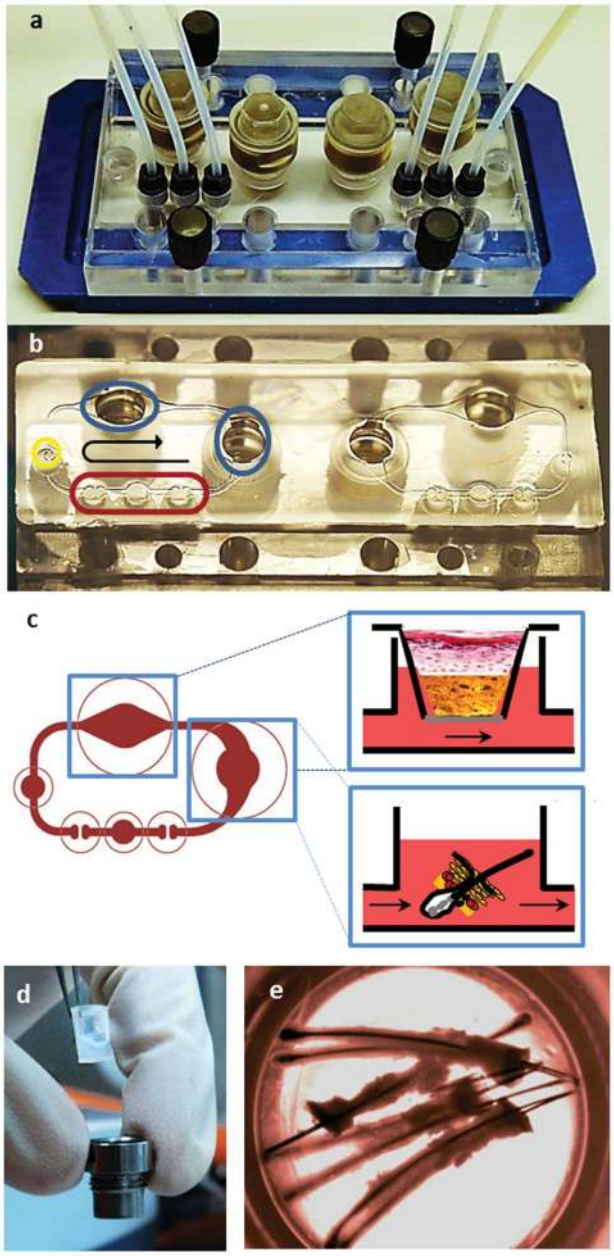

Fig. 1 Multi-organ-chip (MOC). (a) MOC with built-in micropump providing a pulsatile flow of medium. (b) MOC upside down; red circle: built-in micropump region, yellow circle: injection port, blue circles: insert areas compatible with 96well-Transwell® inserts. Black arrow shows the direction of flow. This chip includes two circuits as mirror images. (c) Insert areas are used separately for culturing *ex vivo* SBs and in vitro SEs in Transwells® or FUEs directly in the stream, as shown in the schematic. (d) An SE in a Transwell® insert, being placed in an MOC Transwell® support. (e) FUEs in MOC insert area.

bining an on-chip micropump (Fig. 1b, red circle) with variable tissue culture compartments (Fig. 1b, blue circle, Fig. 1c). The MOC system provides a platform to assess the effect of dynamic perfusion in comparison to common static culture conditions of different skin model systems. It is designed to operate two microfluidic circuits simultaneously. Fig. 1b is a photo of the MOC showing the positioning of the key elements at a glance. The layout of the MOC supports the flexible integration of conventional miniaturised tissue culture formats, such as Transwell® (Corning, Lowell, MA, USA) inserts, special organotypic matrices, or native normal or diseased *ex vivo* biopsies in the tissue culture compartments (Fig. 1c blue rectangles). The micropump is capable of providing a pulsatile flow of medium through 500 μm wide × 100 μm high channels with a pumping volume range of 7–70 μl min^{-1} and a frequency of 0.2–2.5 Hz. We used a frequency of 0.3 Hz in our experiments, which leads to a flow-rate of approximately 30 μl min^{-1}. SEs and skin biopsies (SBs) were each held in a single 96-well Transwell® insert with a surface area of 14.3 mm^2, placed in the insert holders (Fig. 1d) to provide an air–liquid interphase (Fig. 1c), while FUEs were positioned directly into the insert areas leading to submerged culture conditions within the medium stream (Fig. 1c and e). For a detailed description of the MOC assembly procedure, please refer to the work of Wagner and colleagues in this issue.[15]

Tissue sources and culture conditions

We used EpiDermFT™ (Mattek, Ashland, MA, USA) as a full-thickness *in vitro* model for the *in vitro* SE experiments. A 5 mm punch biopsy device (Stusche, Teltow, Germany) was used to adjust the SE's size to the Transwell® (Corning, Lowell, MA, USA) insert. Dulbecco's Modified Eagle's Medium (DMEM)-based maintenance medium (EFT-400-MM, Mattek, Ashland, MA, USA) was used, according to the manufacturer's instructions. A total volume of 500 μl medium was in place, while 200 μl was changed every day during the 9 days of culture for both MOC-based dynamic and static cultures in air–liquid interphase. We used deep Transwell® holder wells for the static cultures, with the same medium volume in all parallel cultures.

Human juvenile prepuce was obtained in compliance with the relevant laws, with informed consent and ethical approval from the Ethics Committee of the Charité Universitätsmedizin, Berlin, Germany, after routine circumcisions from paediatric surgery. The tissue was stored in PBS at +4 °C and processed within 4 h after surgery. Skins were sterilized in 80% ethanol for 30 s and cut open. SCT was removed from the skin and placed underneath the SE, prepared as described above. These combined tissues were positioned in the Transwell® insert and transferred to the respective MOC compartment utilising the same experimental conditions as mentioned above for a duration of 7 days (Fig. 1d).

Similarly, we used juvenile prepuce for the *ex vivo* skin experiments and processed them as described above. Three donors were used for each MOC-based static and dynamic experiment in parallel. The skin was separated from the subcutaneous tissue, punched to 5 mm biopsies, fixed in the Transwell® insert, and transferred to the MOC tissue segment in air–liquid interphase. SBs were supplemented for 14 days in high glucose (4.5 mg ml^{-1}) DMEM with 10% foetal calf serum (FCS), 100 units ml^{-1} penicillin, 100 μg ml^{-1} streptomycin, and L-glutamine. An amount of 200 μl of the total 500 μl of medium was exchanged every day.

Occipital and temporal scalp skin FUEs containing mainly growing anagen VI hair follicles were obtained from disposed excess skin samples derived from male patients aged between

25–55 years undergoing hair transplantation surgery. FUEs were delivered in Williams's E medium with 100 units/ml penicillin and 100 μg ml^{-1} streptomycin, and processed within 4 h after surgery by placing them directly in the microcirculation of the MOC system (Fig. 1c and e). We used William's E medium supplemented with 10% FCS, 100 units/ml penicillin, 100 μg ml^{-1} streptomycin, 5 μg ml^{-1} human insulin, 2 mM L-glutamine, and 5×10^{-5} M hydrocortisone hemisuccinate (Sigma Aldrich, Schnelldorf, Germany) as the culture medium. An amount of 350 μl of a total of 600 μl was exchanged every second day during the 14 days of culture.

Sample preparation, histology and imaging

Samples were removed from Transwells® inserts, placed in Tissue-Tek® OCT™ Compound (Sakura, Alphen aan den Rijn, Netherlands) and subsequently snap frozen for end-point analysis. The tissue blocks were sectioned with a Leica CM1950 Cryostat (Wetzlar, Germany) at 8 μm thickness.

We used standard haematoxylin and eosin (H&E) staining to analyse the sections histologically. Immunofluorescence staining was applied to characterize for tissue-specific markers. Briefly, we used a Ki67 (Abcam, Cambridge, UK) – TUNEL (Apoptag, Millipore, Darmstadt, Germany) double immunovisualisation technique, as described before[16] on cryosections for the detection of proliferating and apoptotic cells. Double immunofluorescence staining with cytokeratin 10 (CK10; Abcam, Cambridge, UK) and cytokeratin 15 (CK15; Abcam, Cambridge, UK) were used for epidermal markers, while Collagen IV (ColIV; Sigma Aldrich, Schnelldorf, Germany) and Tenascin C (TenC; Santa Cruz Biotechnology, Heidelberg, Germany) were visualised for basement membrane and dermis. In addition, pan cytokeratin (an antibody mixture that stains a wide range of different CKs; Sigma Aldrich, Schnelldorf, Germany) and ColIV (Sigma Aldrich, Schnelldorf, Germany) double immunofluorescence staining was applied for hair follicle tissue samples.

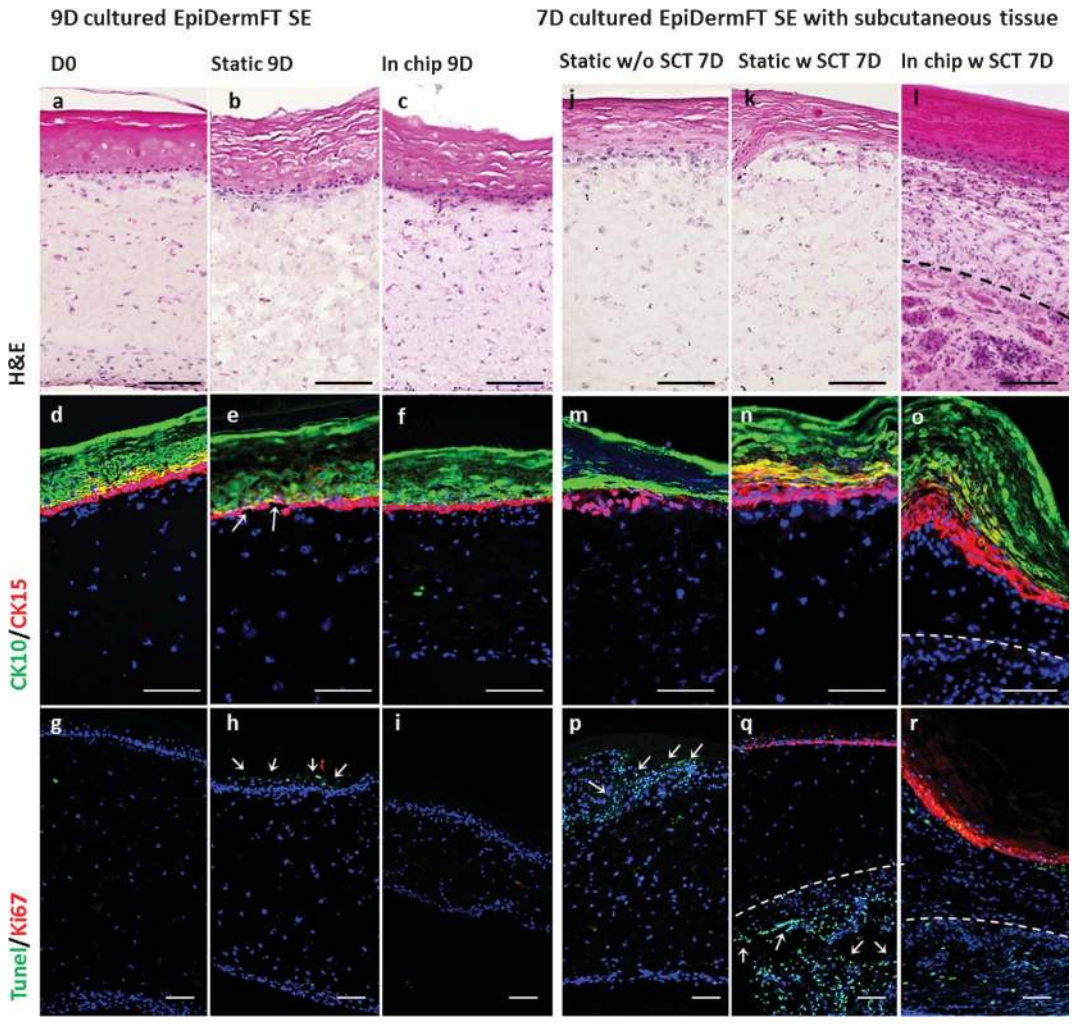

Fig. 2 *In vitro* skin equivalents (Mattek, Ashland, US) cultured for 9 days in MOC or static conditions in comparison to the same SE cultured for 7 days with subcutaneous tissue (SCT) from prepuce. Haematoxylin and eosin (H&E) staining for histological comparison of the sections (a–c, j–l) and immunofluorescence staining for epidermal markers Cytokeratin 10 and 15 (d–f, m–o) are applied. Overlapping markers are visualized as yellow. Finally, Ki67 and TUNEL assay for proliferation and apoptosis (g–i, p–r) are used for comparison of viability of tissues (arrows indicate discontinuous basal layer of epidermis in e, TUNEL positive apoptotic cells in p and disintegrated tissue in q). Dashed lines mark the border between SE and SCT. Scale bars indicate 100 μm for each picture.

A Keyence BZ-9000 Microscope with the BZ-II-Viewer software was used for all microscopic imaging and the images were merged using the BZ-II-Analyser software (Keyence, Neu Isenburg, Germany). Phase contrast and fluorescent images were adjusted for tone levels, brightness and contrast.

Results and discussion

9-day cultured EpiDermFT skin equivalent

We prolonged the recommended culture period for static conditions of EpiDermFT SE to a total culture period of 9 days. We could observe a rearrangement and compression of the dermal matrix structure in dynamic MOC cultures as cell nuclei are located closer to each other with denser extracellular matrix structure compared to day 0 and the control. There were more viable cells in the SEs cultured in the MOC compared to the SEs with static culture conditions (Fig. 2a–c). The different layers of the epidermis were stained by immunofluorescence showing the expression of the epidermal markers CK10 for differentiating keratinocytes and CK15 for undifferentiated keratinocytes. Both were similarly expressed in static and dynamic MOC cultures. Although epidermal barrier function seemed to be preserved better in the MOC culture according to the continuous lining of the CK15 positive cells at the basal layer of the epidermis, there is discontinuity in static culture as indicated with arrows (Fig. 2d–f). Hardly any proliferating and apoptotic cells were seen in the MOC and day 0 control sections according to Ki67 TUNEL double staining (Fig. 2g, i), whereas selected apoptotic cells could be found in the epidermal layer in static cultures (Fig. 2h), suggesting the onset of degradation of this SE.

7-day cultured EpiDermFT skin equivalent with sub-cutaneous tissue

We used EpiDermFT^{TM} SE in combination with SCT dissected from a prepuce. SCT is composed mainly of adipocytes, fibroblasts and macrophages. Considering the support of lipid metabolism and paracrine effects of adipose-derived cells on the upper levels of skin, we integrated SCT to EpiDermFT^{TM} SE under the same experimental conditions for 7 days. We observed more viable cells and a compressed dermal matrix in the samples with SCT cultured in the MOC compared to static cultures with and without SCT stained by H&E (Fig. 2j–l). SCT tissue was well integrated to SE in the MOC (Fig. 2l), while its integration was poor in the static culture (Fig. 2q, arrows indicating disintegrated tissue). CK15 positive cells are more abundant in the MOC culture (Fig. 2o) showing the greatest similarity to the native tissue (Fig. 3d as reference), even though there is an increase of undifferentiated keratinocytes in the static culture with SCT compared to regular static culture (Fig. 2m, n). In contrast to static cultures, proliferating cells are observed at the basal layer of the epidermis in cultures with SCT and even more in the dynamic cultures (Fig. 2p–r). SCT is expected to have a stimulating effect on epidermal cells and this effect seemed to be even more prevalent in the dynamic culture. Considering the absence of proliferating cells in the epidermis in the cultures without

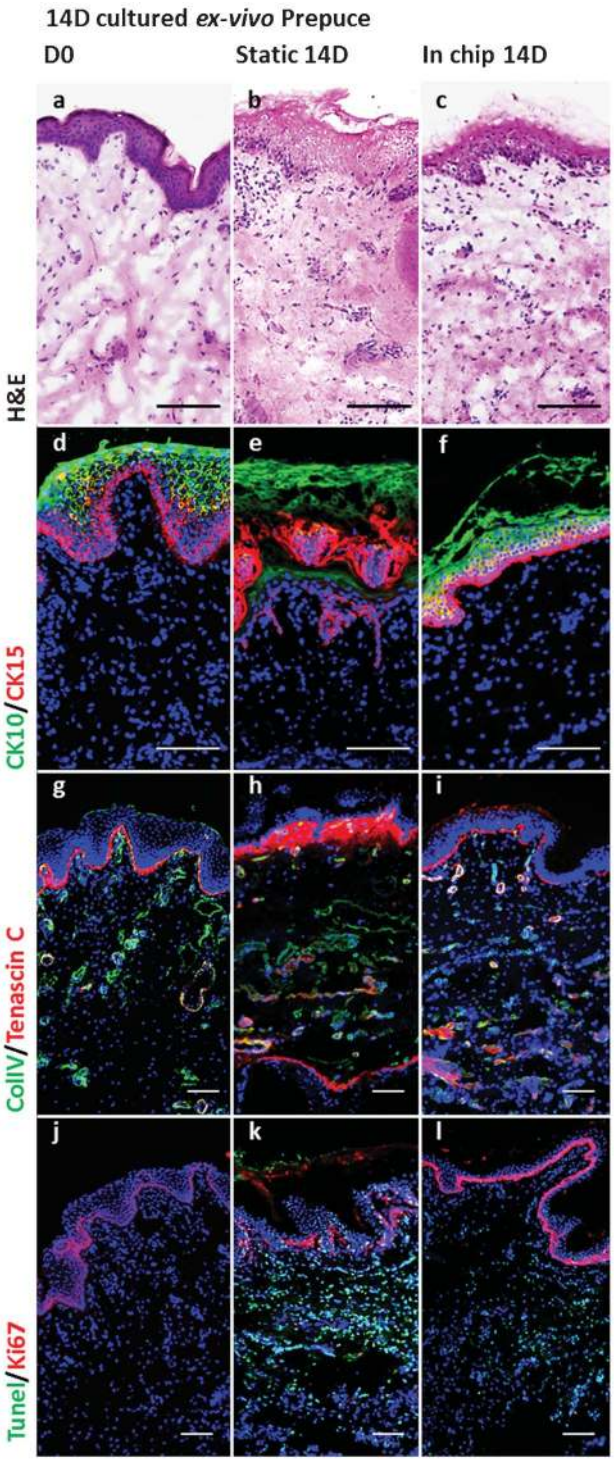

Fig. 3 Maintenance of *ex vivo* prepuce 14 days in culture. Day zero conditions of the tissue are shown in a, d, g, and j. Static cultures are shown in b, e, h, and k, while dynamically cultured tissue in MOC is indicated with c, f, i and l. H&E staining is applied for histological comparison of the tissues (a–c). Immunofluorescence staining for epidermal markers Cytokeratin 10 and 15 (d–f), basement membrane markers Tenascin (TenC) and Collagen IV (ColIV) (g–i), finally, Ki67 and TUNEL assay for proliferation and apoptosis (j–l) are used for the evaluation of the viability of the tissues. Overlapping markers are visualized as yellow. Scale bars indicate 100 μm for each picture.

SCT, epidermal integrity is expected to be weakened (Fig. 2h, p). A massive increase in the amount of apoptotic cells is seen in the SCT of the static culture. The tissue itself is also poorly integrated to the SE (Fig. 2q). Taking these results into account, a higher metabolism of the *ex vivo* tissue seems to require dynamic perfusion.

14-day cultured *ex vivo* prepuce

We evaluated SB maintenance in culture for future substance testing in comparison to SEs. Histological evaluation by H&E showed epidermal disruption and dermal reorganisation in the static cultures (Fig. 3b), whereas MOC-cultured biopsies showed similar distribution to the control tissues (Fig. 3a, c). In addition, CK10/CK15 staining showed a disintegrated epidermis in the static culture compared to day 0 and MOC culture (Fig. 3d–f). ColIV and TenC, which are both synthesised and secreted by keratinocytes and fibroblasts, were used as markers for the extracellular basement membrane.[17] ColIV is mainly found in the basement membrane of the skin, including the epidermal-dermal border and the dermal-endodermal border including blood vessels.[18] TenC is an extracellular matrix component known to be important for cell shape and migration behaviour. It has a pro-migratory role for epidermal cells around the basement membrane in skin and has been shown to be upregulated during wound healing, inflammatory processes and fibrosis.[19,20] For native skin expression pattern of ColIV and TenC, see Fig. 3g. ColIV expression was generally preserved in contrast to TenC (Fig. 3g–i). Static SB culture shows elevated levels of TenC below the basement membrane, suggesting induced fibrotic processes (Fig. 3h). Proliferation in the epidermis was maintained in the MOC according to Ki67 positive cells, while it was decreased in static culture compared to day 0. TUNEL positive cells in dermis are more abundant in the static culture compared to the MOC culture, suggesting a higher amount of cell loss (Fig. 3j–l).

14-day cultured *ex vivo* follicular unit extracts

We used the MOC system to culture FUEs as a further step in the attempt to emulate the biology of the skin and its appendages. In contrast to the well-established Philpott assay using single, truncated hair follicles to study hair follicle biology *in vitro*,[21] we cultured complete hair follicular units. These almost intact philosebaceous units include the perifollicular epidermis, dermis and the sebaceous gland(s). We aimed to prolong the culture period of the *ex vivo* hair follicles, taking into account the support of the glands and the surrounding skin tissue on hair follicle maintenance. H&E staining showed partial loss of structural integrity and a decrease in the total number of cell nuclei within the central and proximal hair follicle after 14 days of culture (Fig. 4a, b), indicating signs of the ongoing regression phase (catagen) of the hair follicle. Nevertheless, a pan cyto-keratin and ColIV double immunostaining revealed an intact appearance of the

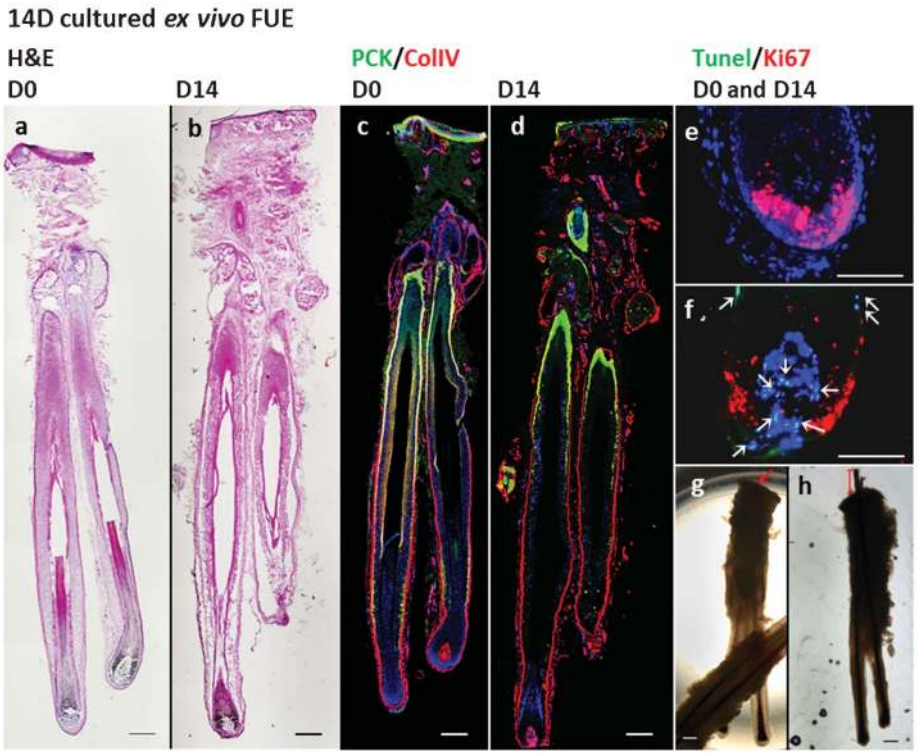

Fig. 4 FUEs cultured in the MOC for 14 days. H&E staining for day 0 and day 14 sample (a, b). Immunofluorescence staining for collective CKs (PCK) and ColIV for day 0 and day 14 samples (c, d) TUNEL assay and Ki67 staining shown for bulb region of the hair for day 0 and day 14 sample (e, f) (arrows indicate TUNEL positive cells in the DP and CTS. Light microscopy images from day 0 and day 14 indicating hairs-shaft elongation in culture (g, h). Scale bars indicate 200 μm for a, b, c and d; 50 μm for e and f; 300 μm for g and h.

basement membrane, connective tissue and dermal papilla of the follicle compared to day 0 (Fig. 4c, d). Although the number of proliferating cells in the follicular bulb surrounding the hair follicle papilla has decreased, numerous Ki67 positive cells are still present after 14 days of culture. Apoptotic cells seen within the dermal papilla and the proximal connective tissue sheath further suggest catagen progression in the hair follicle (Fig. 4f). During the culture period, we observed hair-shaft elongation in growing anagen hair follicles, as depicted in Fig. 4g and 4h. These results suggest that we were able to prolong the culture period of the hair follicle *ex vivo* by dynamic perfusion and postponed the initiation of catagen compared to the Philpott assay.[21]

Conclusions

In general, biophysical and biochemical signals are strongly coupled. Mechanical forces, represented by shear stress in our system, have, for example, influence on the relative distances between cells, ECM components and effector molecules.[22] The flow generated by our perfusion culture system will not only affect the effective distances of signalling molecules and their pericellular diffusion gradients, but could also directly alter extracellular gradients, cell–cell communications and local concentrations of secreted ligands of tissues that were maintained in the MOC. Our results support these positive effects of dynamic perfusion. We were able to prolong the suggested culture period of *in vitro* SE in the MOC. The presence of SCT increased the longevity of the *in vitro* SE in both static and especially in MOC cultures with improved tissue architecture. Native skin has a highly heterogenic nature and comprises cells from three germ layers forming sensory organs, secretory glands and a complex vascular network. Many steps still lie ahead with the current SEs until we reach the complexity of the native organ. For that reason, we cultured *ex vivo* prepuce as a skin organ culture aiming to maintain the native state of the tissue, and our results indicated a distinct difference between the parallel static and MOC cultures, and that tissue disintegration is prevented by dynamic perfusion. Hair follicle cultures in the MOC showed a prominent hair-fibre elongation from the epidermis while tripling the culture period compared to the Philpott assay originally described for *ex vivo* hair elongation and substance testing. These experiments suggest that we are on the right track for simulating skin and hair follicle biology at a miniaturised scale. The MOC bioreactor platform described enables an improved spatiotemporal control of cellular microenvironments compared to traditional *in vitro* assays and is thus capable of short- and mid-term culturing to date and long-term functional organotypic models in the future.

List of abbreviations

MOC	Multi-Organ-Chip
PDMS	Polydimethylsiloxane
SE	skin equivalent
SB	skin biopsy
SCT	subcutaneous tissue
FUE	follicular unit extracts
TUNEL	Terminal deoxynucleotidyl transferase dUTP nick end labeling
H&E	Haematoxylin and eosin
DMEM	Dulbecco's Modified Eagle's Medium
CK	cytokeratin
ColIV	Collagen IV
TenC	Tenascin C.

Acknowledgements

This research was supported by the German Federal Ministry of Education and Research (BMBF; Grant number: 0315569) and the Russian Ministry for Science (Grant number: 16.522.12.2015, 16.522.11.7057). Contributions to B.A. were made possible by DFG funding through the Berlin-Brandenburg School for Regenerative Therapies GSC203. We thank Sven Brincker and Alexandra Lorenz for their technical and Philip Saunders for his creative assistance.

Notes and references

1 R. V. Shevchenko, S. L. James and S. E. James, *J. R. Soc. Interface*, 2010, **7**, 229–58.
2 F. Groeber, M. Holeiter, M. Hampel, S. Hinderer and K. Schenke-Layland, *Adv. Drug Delivery Rev.*, 2011, **63**, 352–66.
3 A. D. Metcalfe and M. W. J. Ferguson, *J. R. Soc. Interface*, 2007, **4**, 413–37.
4 E. Festa, J. Fretz, R. Berry, B. Schmidt, M. Rodeheffer, M. Horowitz and V. Horsley, *Cell*, 2011, **146**, 761–71.
5 G. Lindner, R. Horland, I. Wagner, B. Atac and R. Lauster, *J. Biotechnol.*, 2011, **152**, 108–112.
6 A. F. Black, V. Hudon, O. Damour, L. Germain and F. A. Auger, *Cell Biol. Toxicol.*, 1999, **15**, 81–90.
7 I. Montaño, C. Schiestl, J. Schneider, L. Pontiggia, J. Luginbühl, T. Biedermann, S. Böttcher-Haberzeth, E. Braziulis, M. Meuli and E. Reichmann, *Tissue Eng. A*, 2010, **16**, 269–82.
8 H. Sugihara, S. Toda, N. Yonemitsu and K. Watanabe, *Br. J. Dermatol.*, 2001, **144**, 244–53.
9 J. Lademann, F. Knorr, H. Richter, U. Blume-Peytavi, A. Vogt, C. Antoniou, W. Sterry and A. Patzelt, *Skin Pharmacol. Physiol.*, 2008, **21**, 150–5.
10 F. Knorr, J. Lademann, A. Patzelt, W. Sterry, U. Blume-Peytavi and A. Vogt, *Eur. J. Pharm. Biopharm.*, 2009, **71**, 173–80.
11 S. Tiede, J. E. Kloepper, E. Bodò, S. Tiwari, C. Kruse and R. Paus, *Eur. J. Cell Biol.*, 2007, **86**, 355–76.
12 M. Ponec, A. El Ghalbzouri, R. Dijkman, J. Kempenaar, G. van der Pluijm and P. Koolwijk, *Angiogenesis*, 2004, **7**, 295–305.
13 F. Sonntag, N. Schilling, K. Mader, M. Gruchow, U. Klotzbach, G. Lindner, R. Horland, I. Wagner,

R. Lauster, S. Howitz, S. Hoffmann and U. Marx, *J. Biotechnol.*, 2010, **148**, 70–75.
14 U. Marx, H. Walles, S. Hoffmann, G. Lindner, R. Horland, F. Sonntag, U. Klotzbach, D. Sakharov, A. Tonevitsky and R. Lauster, *Alternatives to laboratory animals : ATLA*, 2012, **40**, 235–57.
15 I. Wagner, E.-M. Materne, S. Brincker, U. Süßbier, C. Frädrich, M. Busek, F. Sonntag, D. A. Sakharov, E. V. Trushkin, A. G. Tonevitsky, R. Lauster and U. Marx, *Lab Chip*, 2013, DOI: 10.1039/c3lc50234a.
16 G. Lindner, A. Menrad, E. Gherardi, G. Merlino, P. Welker, B. Handjiski, B. Roloff and R. Paus, *FASEB J.*, 2000, **14**, 319–32.
17 C. Marionnet, C. Pierrard, C. Vioux-Chagnoleau, J. Sok, D. Asselineau and F. Bernerd, *J. Invest. Dermatol.*, 2006, **126**, 971–9.
18 A. M. Abreu-Velez and M. S. Howard, *North American Journal of Medical Sciences*, 2012, **4**, 1–8.
19 G. P. Sidgwick and A. Bayat, *J. Eur. Acad. Dermatol. Venereol.*, 2012, **26**, 141–152.
20 R. Chiquet-Ehrismann, *Int. J. Biochem. Cell Biol.*, 2004, **36**, 986–90.
21 M. P. Philpott, M. R. Green and T. Kealey, *J. Cell Sci.*, 1990, **97**, 463–71.
22 L. G. Griffith and M. A. Swartz, *Nat. Rev. Mol. Cell Biol.*, 2006, **7**, 211–24.